AIP Physics of Plasmas

Minimum energy states of the cylindrical plasma pinch in single-fluid and Hall magnetohydrodynamics

I. V. Khalzov, F. Ebrahimi, D. D. Schnack, and V. V. Mirnov

Citation: Phys. Plasmas **19**, 012111 (2012); doi: 10.1063/1.3676600
View online: http://dx.doi.org/10.1063/1.3676600
View Table of Contents: http://pop.aip.org/resource/1/PHPAEN/v19/i1
Published by the American Institute of Physics.

Minimum energy states of the cylindrical plasma pinch in single-fluid and Hall magnetohydrodynamics

I. V. Khalzov,[1] F. Ebrahimi,[2] D. D. Schnack,[1] and V. V. Mirnov[1]
[1]*Center for Magnetic Self-Organization, University of Wisconsin, 1150 University Avenue, Madison, Wisconsin 53706, USA*
[2]*University of New Hampshire, 8 College Road, Durham, New Hampshire 03824, USA*

(Received 24 May 2011; accepted 29 November 2011; published online 20 January 2012)

Relaxed states of a plasma column are found analytically in single-fluid and Hall magnetohydrodynamics (MHD). We perform complete minimization of the energy with constraints imposed by invariants inherent in the corresponding models. It is shown that the relaxed state in Hall MHD is a force-free magnetic field with uniform axial flow and/or rigid azimuthal rotation. In contrast, the relaxed states in single-fluid MHD are more complex due to the coupling between velocity and magnetic field. Cylindrically and helically symmetric relaxed states are considered for both models. Helical states may be time dependent and analogous to helical waves, propagating on a cylindrically symmetric background. Application of our results to reversed-field pinches (RFP) is discussed. The radial profile of the parallel momentum predicted by the single-fluid MHD relaxation theory is shown to be in reasonable agreement with experimental observation from the Madison symmetric torus RFP experiment.
[doi:10.1063/1.3676600]

I. INTRODUCTION

Many magnetized plasma systems exhibit the phenomenon of self-organization—the spontaneous tendency to evolve toward preferred configurations with ordered structure. Theoretical prediction of such configurations is a long-standing problem for both laboratory and astrophysical applications. Due to the complexity and nonlinearity of plasma behavior there is no universal mathematical methodology, except direct numerical simulations, that would be able to describe the final self-organized states in all systems.

Among the plasma systems, whose self-organized states can be predicted theoretically, are the systems without external energy supply. In such isolated systems, the process of self-organization is usually referred to as relaxation. The concept of plasma relaxation was proposed by Taylor,[1] who conjectured that during turbulent dynamics a slightly resistive magnetohydrodynamic (MHD) system tends to minimize its magnetic energy while conserving the total magnetic helicity. The underlying basis of this approach is the principle of selective decay of invariants,[1–3] i.e., one or more ideal invariants of the system (conserved in the absence of dissipation) are less susceptible to dissipation than energy and thus can be considered as constants during the relaxation process. Mathematically the relaxation theory is formulated as a variational procedure for obtaining a relaxed state by minimizing the energy subject to constraints.

The Taylor theory has been successfully tested in experiments[4–6] and applied for explaining the magnetic structures in laboratory plasmas such as the reversed-field pinch (RFP), multipinch, and spheromak.[2,3] However, the classical Taylor theory does not include possibility of flows that are ubiquitous in experimentally observed relaxed states. The origin of these flows is not well understood; laboratory plasmas rotate in the toroidal and poloidal directions even in the absence of externally applied torques (intrinsic rotation). Further, the experimental parameters are such that the single-fluid MHD model may not be strictly valid, and the inclusion of the effects of separate ion and electron fluids in the model may be required.

The present work is motivated by the recent progress in plasma velocity measurements in the Madison symmetric torus RFP experiment, which show an abrupt change of the global flows during the relaxation events. Detailed temporal and spatial measurements of flow dynamics indicate significant radial angular momentum transport and flattening of the radial flow profiles.[7]

The goal of the present paper is to determine the minimum energy (relaxed) states for a cylindrical RFP, to analyze the possibility of plasma flows in such states in both standard (single-fluid) and Hall MHD (a two-fluid model with massless electrons), and to elucidate their global properties. Since the RFP has significant fraction of "bad" magnetic curvature caused by poloidal magnetic field, the effect of the toroidal curvature can be ignored. The geometry of periodic cylinder is a good approximation for RFP theory and simulations.[2,3] We employ a variational procedure that includes all ideal invariants inherent in corresponding models. While the experiments are open systems that interact with the external environment through applied voltages, here we consider only closed systems. This is consistent with Taylor's approach,[1,2] which has been reliable for predicting the general properties of relaxed magnetic fields without flow. The fields and flows predicted by the present theory may be relevant to the flows that are observed after the crash phase of sawtooth cycle in the RFP. Of course, we cannot comment on the origin of these flows, only on their relaxed properties.

In the framework of single-fluid MHD, the problem of finding relaxed states with flows in geometries relevant to

RFP is addressed in several papers.[8–11] The relaxed flows in these papers are obtained by including into energy minimization procedure the additional constraints, such as cross helicity and momentum (or its components). It should be emphasized here that the cross helicity is an ideal invariant of incompressible MHD and in some special cases of compressible MHD (e.g., Ref. 8); it is also a rugged invariant during relaxation in the presence of dissipation, which is confirmed by numerical simulations.[12] Energy minimization with the cross helicity constraint in periodic cylinder yields a relaxed state with flow parallel to force-free magnetic field[9] (results are corrected in Ref. 10). In Refs. 8 and 11 in addition to the cross helicity, the total angular momentum is taken into account as a conserved quantity in toroidal geometry. This leads to a relaxed state with combination of parallel flow and rigid toroidal rotation. In present paper, we generalize the results of Refs. 9 and 10 by considering along with the cross helicity the total angular and axial momenta as additional invariants of the cylindrical plasma pinch in incompressible MHD.

The relaxation problem in the framework of Hall MHD is considered in numerous papers.[13–23] In Refs. 13–20, the use of electron and ion helicities as invariants during relaxation is theoretically substantiated and the double-Beltrami structure of the relaxed states in Hall MHD is revealed. References 13, 14, and 19 give several analytical examples of the relaxed states for different geometries. However, these solutions do not correspond to true minimum energy states for fixed electron and ion helicities since the minimization procedure is not completed. This is because the unknown Lagrange multipliers used in the variational procedure are not specified in terms of the initial values of the invariants. A more complete analysis is reported in Ref. 21, where the energy of relaxed states is found in toroidal systems as a function of electron and ion helicities. Although the general solution of the double-Beltrami equation has two eigenfunctions, Ref. 21 uses only one of them. This precludes the possibility of two different spatial scales in the relaxed state (as in Refs. 19, 22, and 23). In Ref. 22, relaxed states are obtained as a linear combination of two orthogonal Beltrami eigenfunctions with eigenvalues λ_1 and λ_2, respectively, and the energy is expressed as a function of electron and ion helicities and eigenvalues λ_1 and λ_2. The next step is to find a pair of eigenvalues (λ_1, λ_2) that minimizes the energy; however, this step is missing in Ref. 22.

The full energy minimization of the incompressible Hall MHD system with fixed electron and ion helicities is completed in Ref. 23 assuming the general geometry and orthogonality of the basis Beltrami vectors (which is not true for cylindrically symmetric states). The result is quite surprising: the relaxed state in Hall MHD is always a force-free magnetic field with no plasma flows, i.e., nothing but the Taylor state. Moreover, the authors of Ref. 23 question the conservation of the ion helicity, arguing that it is not a rugged invariant during relaxation and, therefore, it should not be included into energy minimization procedure. The fact that the ion helicity is not conserved in Hall MHD relaxation is confirmed by numerical simulations.[23–25] In present paper, we extend the results of Ref. 23 for cylindrical plasma pinch in incompressible Hall MHD assuming the conservation of both electron and ion helicities and total angular and axial momenta. These velocity related invariants allows us to obtain a relaxed Hall state with plasma flows.

One of the novel results of our paper is the prediction of non-stationary relaxed states, which have the form of helical waves propagating on a cylindrically symmetric background. Such states are realized in both single-fluid and Hall MHD when some of velocity related invariants are not zero.

The paper is organized as follows. In Sec. II, the invariants of incompressible single-fluid and Hall MHD models are introduced. In Secs. III and IV, the minimum energy states are obtained for corresponding models. In Sec. V, comparison of these states with experimental observations is performed. In Sec. VI, these results are summarized and their application for reversed-field pinches is discussed.

II. STATEMENT OF THE PROBLEM

We consider the problem of finding the minimum energy (relaxed) states of an axially periodic cylindrical plasma pinch, with a periodicity length L (Fig. 1). We assume that plasma is incompressible with spatially uniform density ρ, and it is surrounded by a perfectly conducting shell (flux conserver) of radius a. The incompressibility assumption is relevant to RFP physics due to the fact that relaxation in these systems is provided by tearing modes. These modes are slow on Alfvenic time scale and, therefore, essentially incompressible.[26] Moreover, the resulting incompressible relaxed states are in good agreement with experimental observations, as shown below in Sec. V.

Under these assumptions the plasma is described by equations of ideal incompressible Hall MHD, which in non-dimensional form are[14]

$$\frac{\partial \mathbf{v}}{\partial \tau} + \nabla\left(p + \frac{\mathbf{v}^2}{2}\right) = \mathbf{v} \times (\nabla \times \mathbf{v}) + (\nabla \times \mathbf{b}) \times \mathbf{b}, \nabla \cdot \mathbf{v} = 0, \tag{1}$$

$$\frac{\partial \mathbf{b}}{\partial \tau} = \nabla \times (\mathbf{v} \times \mathbf{b} - \epsilon(\nabla \times \mathbf{b}) \times \mathbf{b}), \nabla \cdot \mathbf{b} = 0. \tag{2}$$

Here, all physical quantities are normalized,

$$r = \frac{R}{a}, \quad z = \frac{Z}{a}, \quad l = \frac{L}{a}, \quad \tau = \frac{V_A}{a}t, \quad \mathbf{v} = \frac{\mathbf{V}}{V_A}, \quad \mathbf{b} = \frac{\mathbf{B}}{B_0}, \quad p = \frac{P}{\rho V_A^2},$$

where the Alfvén velocity V_A and the characteristic magnetic field B_0 are defined as

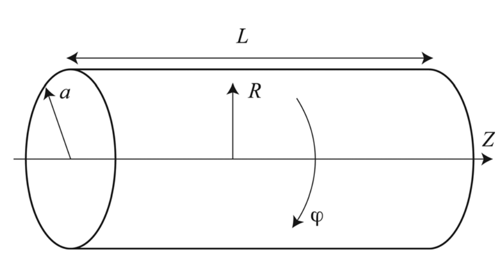

FIG. 1. Geometry of the problem.

$$V_A = \frac{B_0}{\sqrt{4\pi\rho}}, \quad B_0 = \frac{\Phi_0}{\pi a^2}, \tag{3}$$

with Φ_0 being a total axial magnetic flux, which is constant due to perfectly conducting boundary. Equations (1) and (2) also contain the non-dimensional ion skin depth (or Hall parameter) ϵ, which is defined as

$$\epsilon = \frac{d_i}{a} = \frac{c}{a}\sqrt{\frac{m_i^2}{4\pi\rho e^2 Z^2}}, \tag{4}$$

where m_i and eZ are ion mass and charge, c is speed of light. In the limit $\epsilon \to 0$, single-fluid MHD is recovered.

We adopt cylindrical coordinate system $\{r, \varphi, z\}$ with volume element $d^3\mathbf{r} = r dr\, d\varphi\, dz$. In order to solve Eqs. (1) and (2) uniquely, we have to specify boundary conditions for velocity and magnetic field. At an impermeable surface the normal component of velocity vanishes,

$$v_r\Big|_{r=1} = 0, \tag{5}$$

and the normal component of magnetic field and the tangential component of electric field are zero at the perfectly conducting boundary, which is equivalent to

$$b_r\Big|_{r=1} = 0, \quad \epsilon j_r\Big|_{r=1} = 0, \tag{6}$$

where $\mathbf{j} = \nabla \times \mathbf{b}$ is normalized current density. Note that in single-fluid MHD ($\epsilon = 0$) the second condition in Eq. (6) is satisfied automatically.

According to the fundamental idea of the Taylor theory, a weakly dissipative system reaches a state of minimum energy without significant change of certain global quantities. These quantities usually correspond to ideal invariants; they are conserved in ideal system and decay slowly (slower than energy) in presence of dissipation. A number of these ideal invariants inherent in system [Eqs. (1) and (2)] have been introduced into analysis.[1,9,11,13,14] In this section, we examine these invariants for cylindrical pinch geometry assuming boundary conditions [Eqs. (5) and (6)].

The sum of the kinetic and magnetic energies,

$$E = \frac{1}{2}\int (\mathbf{v}^2 + \mathbf{b}^2) d^3\mathbf{r}, \tag{7}$$

is an ideal invariant in the incompressible closed system. Indeed, its time derivative is reduced to a surface integral,

$$\frac{\partial E}{\partial \tau} = -\int_S \left[\left(p + \frac{\mathbf{v}^2}{2}\right)\mathbf{v} + \mathbf{b} \times (\mathbf{v} \times \mathbf{b} - \epsilon \mathbf{j} \times \mathbf{b})\right] \cdot d\mathbf{S},$$

which is zero for boundary conditions [Eqs. (5) and (6)]. In a dissipative incompressible closed system, energy E can only decrease in time. This validates the procedure of energy minimization in relaxation theory.

Magnetic helicity I_1 is equivalent to electron helicity H_e for massless electrons,

$$I_1 \equiv H_e = \int \mathbf{A} \cdot \nabla \times \mathbf{A} d^3\mathbf{r}, \quad I_1\Big|_{\tau=0} = \pi l K. \tag{8}$$

Here $\mathbf{A}$ is vector potential, such that $\mathbf{b} = \nabla \times \mathbf{A}$. The time dynamics of vector potential follows from Eq. (2):

$$\frac{\partial \mathbf{A}}{\partial \tau} = -\nabla\phi + \mathbf{v} \times \mathbf{b} - \epsilon(\nabla \times \mathbf{b}) \times \mathbf{b},$$

where ϕ is normalized electric potential. As a result, the time derivative of magnetic helicity is

$$\frac{\partial I_1}{\partial \tau} = -\int_S (\phi \mathbf{b} + \mathbf{A} \times (\mathbf{v} \times \mathbf{b} - \epsilon \mathbf{j} \times \mathbf{b})) \cdot d\mathbf{S},$$

which is zero if electric potential ϕ is periodic in z and boundary conditions [Eqs. (5) and (6)] are satisfied. Therefore, magnetic helicity is an ideal invariant; it can change only in presence of resistivity. For our study it is important that in resistive systems magnetic helicity is more robust than the energy,[1–3] i.e., we can assume that its value is approximately constant in time and equal to its initial value, $I_1 = \pi l K$, where πl is dimensionless volume of the cylinder and K is the volume-averaged density of the magnetic helicity. For unique definition of vector potential and, therefore, magnetic helicity we use a gauge invariance condition[27]

$$\int_0^l A_z\Big|_{r=1} dz = 0. \tag{9}$$

Single-fluid incompressible MHD system ($\epsilon = 0$) has the well-known ideal invariant–cross helicity,

$$I_2 = \int \mathbf{v} \cdot \mathbf{b}\, d^3\mathbf{r}, \quad I_2\Big|_{\tau=0} = \pi l M. \tag{10}$$

Indeed, its time derivative is

$$\frac{\partial I_2}{\partial \tau} = -\int_S \left[\left(p + \frac{\mathbf{v}^2}{2}\right)\mathbf{b} + \mathbf{v} \times (\mathbf{v} \times \mathbf{b})\right] \cdot d\mathbf{S},$$

which is zero for boundary conditions [Eqs. (5) and (6)]. Cross helicity can be considered also as a rugged invariant (approximately conserved quantity) during relaxation. Its ruggedness in a dissipative single-fluid MHD system is confirmed by numerical simulations for cases, where relaxation is slow on Alfvenic time scales[12]—typical situation for RFP experiments, in which relaxation is provided by slow tearing modes.[3] In our single-fluid MHD analysis, we assume that the cross helicity is constant and equal to its initial value, $I_2 = \pi l M$.

The analogue of the cross helicity in incompressible Hall MHD ($\epsilon \neq 0$) is generalized cross helicity,

$$\hat{I}_2 = \int \mathbf{v} \cdot (\mathbf{b} + \frac{\epsilon}{2}\nabla \times \mathbf{v}) d^3\mathbf{r}, \quad \hat{I}_2\Big|_{\tau=0} = \pi l \hat{M}. \tag{11}$$

It is related to ion helicity

$$H_i = \int (\mathbf{A} + \epsilon \mathbf{v}) \cdot \nabla \times (\mathbf{A} + \epsilon \mathbf{v}) d^3\mathbf{r}$$

by the equation

$$H_i = H_e + 2\epsilon\hat{I}_2 + \epsilon\int_S (\mathbf{v}\times\mathbf{A})\cdot d\mathbf{S}.$$

Their time derivatives are, respectively,

$$\frac{\partial\hat{I}_2}{\partial\tau} = -\int_S\Big[p\mathbf{b} + \mathbf{v}\times(\mathbf{v}\times\mathbf{b}) + \frac{\epsilon}{2}(p\boldsymbol{\omega} + \mathbf{v}\times(\mathbf{v}\times\boldsymbol{\omega}) - \mathbf{v}\times(\mathbf{j}\times\mathbf{b}))\Big]\cdot d\mathbf{S},$$

$$\frac{\partial H_i}{\partial\tau} = -\int_S\Big[\Big(\phi + \epsilon\Big(p + \frac{\mathbf{v}^2}{2}\Big)\Big)(\mathbf{b}+\epsilon\boldsymbol{\omega}) + (\mathbf{A}+\epsilon\mathbf{v})\times(\mathbf{v}\times(\mathbf{b}+\epsilon\boldsymbol{\omega}))\Big]\cdot d\mathbf{S},$$

where $\boldsymbol{\omega} = \nabla\times\mathbf{v}$ is the fluid vorticity. Taking into account boundary conditions [Eqs. (5) and (6)], time derivatives of the generalized cross helicity and ion helicity become

$$\frac{\partial\hat{I}_2}{\partial\tau} = \frac{\epsilon}{2}\int_S\Big(\frac{\mathbf{v}^2}{2} - p\Big)\boldsymbol{\omega}\cdot d\mathbf{S},$$

$$\frac{\partial H_i}{\partial\tau} = \epsilon\int_S\Big(\mathbf{v}\cdot\mathbf{A} - \phi + \epsilon\Big(\frac{\mathbf{v}^2}{2} - p\Big)\Big)\boldsymbol{\omega}\cdot d\mathbf{S}.$$

From these equations one can see that in order for $\hat{I}_2$ and H_i to be conserved, an extra boundary condition must be imposed,[14] which is

$$\omega_r\Big|_{r=1} = 0. \tag{12}$$

This condition is satisfied automatically for all time if it is satisfied initially at $\tau = 0$. This is guaranteed by boundary conditions [Eqs. (5) and (6)] and by equation of ideal dynamics of the fluid vorticity

$$\frac{\partial\boldsymbol{\omega}}{\partial\tau} = \nabla\times(\mathbf{v}\times\boldsymbol{\omega} + \mathbf{j}\times\mathbf{b}), \tag{13}$$

which is obtained from Eq. (1) by taking the curl. In the following, we assume that the generalized cross helicity (and, hence, the ion helicity) is conserved during relaxation and its value is $\hat{I}_2 = \pi l\hat{M}$. As we show in Sec. IV, relaxed state in incompressible Hall MHD is completely independent of this invariant: energy minimizations with or without generalized cross helicity lead to the same result.

Equations (2) and (13) being similar in structure also guarantee the conservation of the axial fluxes of the magnetic field and the fluid vorticity, respectively,

$$I_3 = \int_0^{2\pi}\int_0^1 b_z r dr d\varphi, \quad I_3\Big|_{\tau=0} = \pi, \tag{14}$$

$$I_4 = \int_0^{2\pi}\int_0^1 \omega_z r dr d\varphi = \int_0^{2\pi} v_\varphi\Big|_{r=1} d\varphi, \quad I_4\Big|_{\tau=0} = 2\pi\Omega_b, \tag{15}$$

where we used normalization [Eq. (3)] and assumed that the azimuthally averaged angular velocity at the boundary is Ω_b. Their time derivatives are

$$\frac{\partial I_3}{\partial\tau} = \int_0^{2\pi}(\mathbf{v}\times\mathbf{b} - \epsilon\mathbf{j}\times\mathbf{b})\Big|_{r=1}\cdot\mathbf{e}_\varphi d\varphi,$$

$$\frac{\partial I_4}{\partial\tau} = \int_0^{2\pi}(\mathbf{v}\times\omega + \mathbf{j}\times\mathbf{b})\Big|_{r=1}\cdot\mathbf{e}_\varphi d\varphi.$$

Note that magnetic flux [Eq. (14)] is constant in both single-fluid and Hall MHD due to boundary conditions [Eqs. (5) and (6)], while fluid vorticity flux [Eq. (15)] is conserved only in Hall MHD when additional condition [Eq. (12)] is satisfied.

The geometrical symmetry of the pinch configuration yields two more ideal invariants, the axial and angular momenta,

$$I_5 = \int v_z d^3\mathbf{r}, \quad I_5\Big|_{\tau=0} = \pi l u, \tag{16}$$

$$I_6 = \int r v_\varphi d^3\mathbf{r}, \quad I_6\Big|_{\tau=0} = \frac{\pi l\Omega}{2}. \tag{17}$$

Their time derivatives are zeros for boundary conditions [Eqs. (5) and (6)] since

$$\frac{\partial I_5}{\partial\tau} = \int_S (b_z\mathbf{b} - v_z\mathbf{v})\cdot d\mathbf{S},$$

$$\frac{\partial I_6}{\partial\tau} = \int_S (r b_\varphi\mathbf{b} - r v_\varphi\mathbf{v})\cdot d\mathbf{S}.$$

The initial values of these invariants can always be attributed to some uniform flow with velocity u in z-direction and a rigid rotation with angular velocity Ω in φ-direction.

In the following, we use these invariants as constraints in energy minimization procedure.

III. RELAXED STATES IN SINGLE-FLUID MHD

In this section, we study single-fluid MHD ($\epsilon = 0$) relaxed states. We consider two cases here: the most general case, where relaxed state corresponds to a minimum of energy [Eq. (7)] subject to constraints given by Eqs. (8), (10), (14), (16), and (17); and the case, where we ignore axial and angular momenta constraints given by Eqs. (16) and (17) for the reasons explained below.

A. Energy minimization with full set of invariants

First we consider the case, where relaxed state is found by minimizing energy [Eq. (7)] with the most general set of invariants [Eqs. (8), (10), (14), (16), and (17)] inherent in incompressible single-fluid MHD in periodic cylinder. The Lagrange multipliers method results in variational problem,

$$\delta\Big[E + \mu_1(I_1 - \pi l K) + \mu_2(I_2 - \pi l M) + \mu_3(I_3 - \pi) + \mu_5(I_5 - \pi l u) + \mu_6\Big(I_6 - \frac{\pi l\Omega}{2}\Big)\Big] = 0, \tag{18}$$

which determines a conditional extremum of E (it is minimum since E is positive definite, and, therefore, the resulting equilibrium is ideally stable). The Euler equations of variational problem [Eq. (18)] are

$$\sim \delta \mathbf{v}: \quad \mathbf{v}_0 + \mu_2 \mathbf{b}_0 + \mu_5 \mathbf{e}_z + \mu_6 r \mathbf{e}_\varphi = 0, \tag{19}$$

$$\sim \delta \mathbf{A}: \quad \nabla \times \mathbf{b}_0 + 2\mu_1 \mathbf{b}_0 + \mu_2 \nabla \times \mathbf{v}_0 = 0, \tag{20}$$

$$\sim \delta \mu_k: \quad I_1 = \pi l K, \quad I_2 = \pi l M, \quad I_3 = \pi, \quad I_5 = \pi l u, \quad I_6 = \frac{\pi l \Omega}{2}. \tag{21}$$

Equations (19) and (20) can be reduced to one equation for magnetic field

$$\nabla \times \mathbf{b}_0 - \lambda \mathbf{b}_0 = \frac{2\mu_2 \mu_6}{1-\mu_2^2} \mathbf{e}_z, \tag{22}$$

where

$$\lambda = \frac{2\mu_1}{\mu_2^2 - 1}.$$

Thus, the relaxed magnetic field is no longer force-free as in classical Taylor theory due to its coupling with the relaxed flow. Note that the amplitude of the magnetic field $\mathbf{b}_0$ and the Lagrange multipliers μ_1, μ_2, μ_5, μ_6 are not arbitrary, they are determined by constraints from Eq. (21). Therefore, the relaxed state depends only on the initial values of the invariants.

The most general solution to Eqs. (19) and (20) satisfying gauge invariance condition [Eq. (9)] and constraints $I_3 = \pi$, $I_5 = \pi l u$, $I_6 = \pi l \Omega/2$ is a superposition of a cylindrically symmetric mode (with the azimuthal mode number $m = 0$ and the axial wave-number $k_z = 0$) and modes with $m \neq 0$ or $k_z \neq 0$,

$$\mathbf{A}_0 = \frac{r}{2}\mathbf{e}_\varphi + \frac{C}{\lambda}\left[(J_1(\lambda r) - J_1(\lambda) r)\mathbf{e}_\varphi + (J_0(\lambda r) - J_0(\lambda))\mathbf{e}_z \right] + \frac{1}{\lambda}\mathbf{H}, \tag{23}$$

$$\mathbf{b}_0 = \nabla \times \mathbf{A}_0 = \mathbf{e}_z + C\left[J_1(\lambda r)\mathbf{e}_\varphi + \left(J_0(\lambda r) - \frac{2J_1(\lambda)}{\lambda} \right)\mathbf{e}_z \right] + \mathbf{H}, \tag{24}$$

$$\mathbf{v}_0 = \Omega r \mathbf{e}_\varphi + u \mathbf{e}_z - \mu_2 C\left[\left(J_1(\lambda r) - \frac{4J_2(\lambda)}{\lambda} r \right)\mathbf{e}_\varphi + \left(J_0(\lambda r) - \frac{2J_1(\lambda)}{\lambda} \right)\mathbf{e}_z \right] - \mu_2 \mathbf{H}, \tag{25}$$

where J denotes Bessel functions of the first kind, coefficient C is

$$C = \frac{\lambda(1-\mu_2^2) - 2\Omega\mu_2}{2J_1(\lambda) + 2\mu_2^2 J_3(\lambda)},$$

and $\mathbf{H}$ represents the helical part of the solution (modes with $m \neq 0$ or $k_z \neq 0$), such that $\nabla \times \mathbf{H} = \lambda \mathbf{H}$. Substituting these expressions into Eqs. (7), (8), and (10), we obtain the volume-averaged densities of the energy, the magnetic helicity and the cross helicity,

$$\frac{E}{\pi l} = \frac{1}{2} + \frac{u^2}{2} + \frac{\Omega^2}{4} + \frac{(1+\mu_2^2)C^2}{2}(2J_1^2(\lambda) - 3J_0(\lambda)J_2(\lambda) - J_2^2(\lambda)) - \frac{4\mu_2^2 C^2 J_2^2(\lambda)}{\lambda^2} + \frac{(1+\mu_2^2)D}{2}, \tag{26}$$

$$K = \frac{2C J_2(\lambda)}{\lambda} + \frac{2C^2}{\lambda}(J_1^2(\lambda) - 2J_0(\lambda)J_2(\lambda) - J_2^2(\lambda)) + \frac{D}{\lambda}, \tag{27}$$

$$M = u + \frac{2\Omega C J_2(\lambda)}{\lambda} - \mu_2 C^2\left(2J_1^2(\lambda) - 3J_0(\lambda)J_2(\lambda) - J_2^2(\lambda) - \frac{8J_2^2(\lambda)}{\lambda^2} \right) - \mu_2 D, \tag{28}$$

where D is a non-negative quantity characterizing magnitude of the helical part,

$$D = \frac{1}{\pi l}\int \mathbf{H}^2 d^3\mathbf{r}. \tag{29}$$

Consider first the cylindrically symmetric solution with $D = 0$. In this case Eqs. (27) and (28) are used to find μ_2 and λ through the initial values of helicities, K and M. The resulting volume-averaged energy density of the relaxed state $E_{cs} = (E/\pi l)_{D=0}$ as a function of K is shown in Fig. 2. A sample of the relaxed state with non-zero plasma flows is shown in Fig. 3. It should be emphasized here that the cylindrically symmetric MHD relaxed states are always ideal equilibria, i.e., they satisfy Eqs. (1) and (2) with $\partial/\partial\tau = 0$.

The helical part of the solution $\mathbf{H}$ corresponding to $D \neq 0$ can be presented as a linear combination of modes with non-zero azimuthal mode numbers m and/or axial wave numbers $k_z = \pi n/l$ (m and n are integer),

$$\mathbf{h}_{\lambda,m,k_z} = \frac{m\lambda J_m(\alpha r) + k_z \alpha r J_m'(\alpha r)}{\alpha^2 r}\cos(m\varphi + k_z z + \theta)\mathbf{e}_r - \frac{m k_z J_m(\alpha r) + \lambda \alpha r J_m'(\alpha r)}{\alpha^2 r}\sin(m\varphi + k_z z + \theta)\mathbf{e}_\varphi + J_m(\alpha r)\sin(m\varphi + k_z z + \theta)\mathbf{e}_z, \tag{30}$$

where $\alpha = \sqrt{\lambda^2 - k_z^2}$ is a radial wave-number, θ is an arbitrary phase, and $\nabla \times \mathbf{h}_{\lambda,m,k_z} = \lambda \mathbf{h}_{\lambda,m,k_z}$ by definition. Each helical mode given by Eq. (30) should satisfy boundary condition [Eq. (6)] resulting in

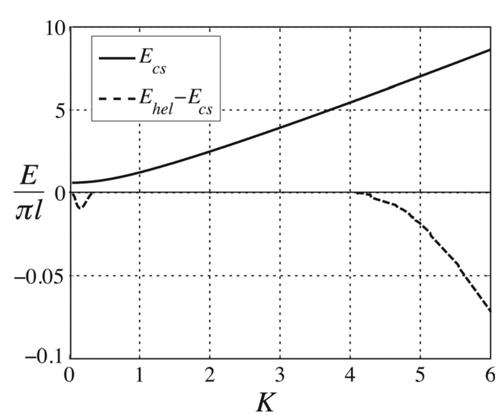

FIG. 2. Volume-averaged energy density of cylindrically symmetric MHD relaxed state [Eqs. (23)–(25)] E_{cs} as a function of magnetic helicity K (solid curve) and its difference with energy density of helically distorted MHD relaxed state E_{hel} in domain of its existence (dashed curve). Note different scales for positive and negative energies. Results are presented for cross helicity $M = 0.1$, axial momentum $u = 0$, angular momentum $\Omega = 0$ and $\lambda = 3.11$ for helical state.

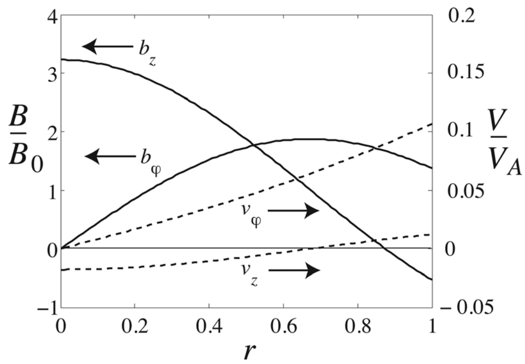

FIG. 3. Cylindrically symmetric MHD relaxed state [Eqs. (23)–(25)] with magnetic helicity $K = 2$, cross helicity $M = 0.1$, axial momentum $u = 0$, and angular momentum $\Omega = 0.1$. Solid lines are components of magnetic field (left vertical axis) and dashed lines are components of velocity (right vertical axis).

$$m\lambda J_m(\alpha) + k_z \alpha r J_m'(\alpha) = 0. \tag{31}$$

For given m and k_z, this equation determines λ (Fig. 4). Note that only one value of λ is possible in the relaxed state as can be seen from Eq. (22). The description of the helically distorted relaxed state is completed by expressing its magnitude D and the Lagrange multiplier μ_2 from Eqs. (27) and (28) in terms of the initial values of helicities, K and M. Our calculations show that in the domain of its existence the helically distorted state has lower energy $E_{hel} = (E/\pi l)_{D>0}$ than the cylindrically symmetric state (Fig. 2); besides, the lowest energy is achieved when the value of λ is minimal. This minimal value $\lambda = 3.11$ corresponds to helical mode with $m = 1$ and $k_z = 1.23$ (Fig. 4); in our following analysis we assume that the helical distortion is due to this mode, i.e.,

$$\mathbf{H} = C_h \mathbf{h}\Big|_{\lambda=3.11,\ m=1,\ k_z=1.23}. \tag{32}$$

The quantity D defined in Eq. (29) can be expressed in terms of the amplitude of the helical distortion C_h,

$$D = \frac{C_h^2 \lambda^2 J_m^2(\alpha)}{\alpha^2}\left(1 + \frac{m^2}{k_z^2} - \frac{m\lambda}{k_z \alpha^2}\right). \tag{33}$$

The domains occupied by cylindrically symmetric and helically distorted relaxed states in the $K - M$ plane are

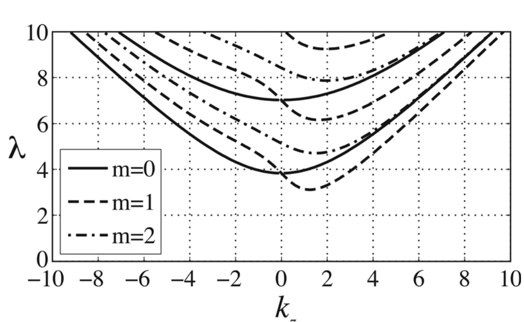

FIG. 4. Eigenvalues λ of helical modes [Eq. (31)] with different azimuthal mode numbers m and axial wave numbers k_z. For periodic cylinder of finite periodicity l, the axial wave numbers are discrete: $k_z = 2\pi n/l$, where n is integer.

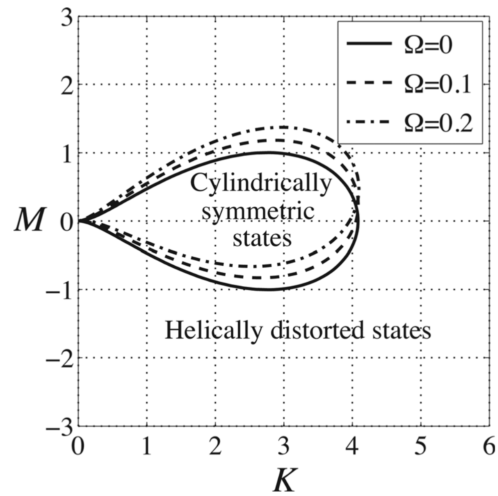

FIG. 5. Domains occupied by cylindrically symmetric and helically distorted MHD relaxed states [Eqs. (23)–(25)] in the plane $K - M$ (magnetic helicity−cross helicity) for axial momentum $u = 0$ and different values of angular momentum Ω.

presented in Fig. 5, the boundary between them can be determined by setting $D = 0$ in Eqs. (27) and (28). The classical force-free Taylor state corresponds to the line $M = 0$ in this figure; it becomes helically distorted for values of magnetic helicity larger than $K = 4.08$, which is in agreement with Ref. 28.

The interesting property of the helically distorted relaxed MHD states is their oscillatory nature. Indeed, substituting Eqs. (24), (25), (30), and (32) in Eqs. (1) and (2) with $\epsilon = 0$ one obtains that the phase θ of the helical distortion is changing with time as

$$\begin{aligned}\frac{\partial\theta}{\partial\tau} &= -\mathbf{k}\cdot(\mathbf{v}_0 + \mu_2 \mathbf{b}_0) \\ &= -m\left(\Omega + \frac{4\mu_2 C J_2(\lambda)}{\lambda}\right) - k_z(u + \mu_2),\end{aligned} \tag{34}$$

where $\mathbf{k} = m/r\mathbf{e}_\varphi + k_z \mathbf{e}_z$ is the wave-vector. In other words, the non-cylindrical part of the relaxed MHD state is the helical wave, which is propagating with a phase velocity $\mathbf{v}_{ph} = \mathbf{v}_0 + \mu_2 \mathbf{b}_0$. At each point of the fluid, relaxed velocity and magnetic field are oscillating near the cylindrically symmetric state with the frequency $\omega = \partial\theta/\partial\tau$ (Fig. 6).

Fig. 7, shows the $F - \Theta$ diagram of the relaxed MHD states with different values of cross helicity M and angular momentum Ω. The reversal parameter F and pinch Θ are defined here as

$$F \equiv \frac{\langle B_z|_{R=a}\rangle_{\varphi,z}}{B_0} = 1 - CJ_2(\lambda), \tag{35}$$

$$\Theta \equiv \frac{\langle B_\varphi|_{R=a}\rangle_{\varphi,z}}{B_0} = CJ_1(\lambda), \tag{36}$$

where brackets $\langle\rangle_{\varphi,z}$ denote averaging over φ and z. As follows from Fig. 7, the presence of the initial flow (non-zero cross helicity M or total angular momentum Ω) in cylindrical plasma pinch affects the relaxed magnetic field significantly. This is due to the coupling of the velocity and the magnetic

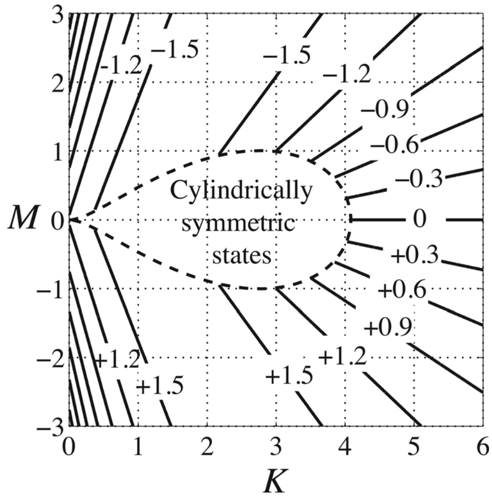

FIG. 6. Values of oscillation frequency $\omega = \partial\theta/\partial\tau$ [Eq. (34)] of the helical distortion in the plane $K - M$ (magnetic helicity−cross helicity) for MHD relaxed state [Eqs. (23)–(25)] with axial momentum $u = 0$ and angular momentum $\Omega = 0$.

field that occurs in Eq. (22) through the term on the right hand side. Such coupling does not take place in the systems without axial symmetry where the angular momentum is not conserved, e.g., in a periodic rectangular box. In this case, a relaxed magnetic field corresponds to a force-free Taylor state and it has the same structure independent of the initial flows and determined by the value of magnetic helicity only.[24,25]

B. Energy minimization without momenta invariants

In order to obtain a relaxed state, which more realistically reflects the features of RFP, we have to exclude both axial I_5 and angular I_6 momenta invariants [Eqs. (16) and (17), respectively] from the energy minimization procedure for the following reasons. The angular momentum invariant I_6 is an artifice of the idealized geometry of periodic cylinder, it does not have an analogue in toroidal systems such as RFP. Although the axial momentum invariant I_5 has a counterpart in toroidal systems, we also discard it because it is not conserved in RFP experiment.[7] Such "fragility" of the

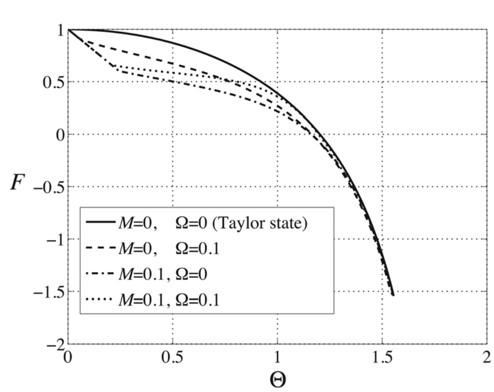

FIG. 7. Reversal parameter F [Eq. (35)] vs. pinch Θ [Eq. (36)] for the relaxed MHD states [Eqs. (23)–(25)] with axial momentum $u = 0$, different values of cross helicity M and angular momentum Ω. The initial straight intervals and the final point of the graphs ($\Theta = 1.55$, $F = -1.55$) correspond to helically distorted states.

axial momentum invariant I_5 in real experiment can be explained by an important role of the viscous dissipation due to no-slip condition at the radial boundary. Results of this subsection reproduce in part results from Ref. 9 with corrections in Ref. 10.

The Euler equations describing a single-fluid MHD relaxed state under these assumptions are

$$\sim \delta\mathbf{v}: \quad \mathbf{v}_0 + \mu_2 \mathbf{b}_0 = 0, \tag{37}$$

$$\sim \delta\mathbf{A}: \quad \nabla\times\mathbf{b}_0 + 2\mu_1\mathbf{b}_0 + \mu_2\nabla\times\mathbf{v}_0 = 0, \tag{38}$$

$$\sim \delta\mu_k: \quad I_1 = \pi l K,\ I_2 = \pi l M,\ I_3 = \pi. \tag{39}$$

Equations (37) and (38) lead to one equation for a relaxed magnetic field,

$$\nabla\times\mathbf{b}_0 = \lambda\mathbf{b}_0, \quad \lambda = \frac{2\mu_1}{\mu_2^2 - 1}, \tag{40}$$

which means that magnetic field relaxes to a force-free Taylor state. Notable feature of this relaxed state is that the flow is parallel to the magnetic field as seen from Eq. (37). The radial structure of this relaxed state is given by

$$\mathbf{A}_0 = \frac{1}{2J_1(\lambda)}[J_1(\lambda r)\mathbf{e}_\varphi + (J_0(\lambda r) - J_0(\lambda))\mathbf{e}_z] + \frac{C_h\mathbf{h}}{\lambda}, \tag{41}$$

$$\mathbf{b}_0 = \nabla\times\mathbf{A}_0 = \frac{\lambda}{2J_1(\lambda)}[J_1(\lambda r)\mathbf{e}_\varphi + J_0(\lambda r)\mathbf{e}_z] + C_h\mathbf{h}, \tag{42}$$

$$\mathbf{v}_0 = -\mu_2\mathbf{b}_0 = -\frac{\mu_2\lambda}{2J_1(\lambda)}[J_1(\lambda r)\mathbf{e}_\varphi + J_0(\lambda r)\mathbf{e}_z] - \mu_2 C_h\mathbf{h}, \tag{43}$$

where helical part of the solution $\mathbf{h}$ is defined in Eq. (30). Here, the parameter λ (for cylindrically symmetric state) or amplitude of the helical part C_h (for helically distorted state) have to be specified from the magnetic helicity constraint, $I_1 = \pi l K$, while Lagrange multiplier μ_2 is determined from the cross helicity constraint, $I_2 = \pi l M$,

$$K = \frac{\lambda}{2}\left(1 - \frac{J_0(\lambda)J_2(\lambda)}{J_1^2(\lambda)}\right) + \frac{D}{\lambda}, \tag{44}$$

$$W \equiv \frac{1}{2\pi l}\int \mathbf{b}_0^2\, d\mathbf{r}^3 = \frac{\lambda^2}{4}\left(1 - \frac{J_0(\lambda)J_2(\lambda)}{J_1^2(\lambda)}\right) + \frac{\lambda J_0(\lambda)}{4J_1(\lambda)} + \frac{D}{2}, \tag{45}$$

$$\mu_2 = -\frac{M}{2W}, \tag{46}$$

where D is magnitude of the helical distortion given by Eq. (33) and W is volume-averaged magnetic energy of the relaxed state. The sum of kinetic and magnetic energy of the state is

$$E = (1 + \mu_2^2)W = W + \frac{M^2}{4W}. \tag{47}$$

Therefore, for relatively small values of cross helicity M the system in many aspects is similar to the classical Taylor relaxed state. In particular, the transition to a helically distorted relaxed state occurs if value of magnetic helicity is larger than $K = 4.08$; the helical state in this case has the lowest possible value of $\lambda = 3.11$ corresponding to $m = 1$ and $k_z = 1.23$. This situation is violated when the cross helicity M is comparable to the magnetic energy W of the relaxed state. In fact, if $M > 2W$ then the minimum energy state is cylindrically symmetric (Fig. 8).

In contrast to the relaxed states from Sec. III A, the states described by Eqs. (41)–(43) are always stationary and do not possess traveling helical waves.

IV. RELAXED STATES IN HALL MHD

In this section, we consider the Hall MHD ($\epsilon \neq 0$) relaxed states corresponding to a minimum of energy [Eq. (7)] subject to constraints given by Eqs. (8), (11), and (14)-(17). As in Sec. III, we follow the standard procedure of minimization by applying the Lagrange multipliers method. Then the Euler equations of variational problem are

$$\sim \delta\mathbf{v} : \mathbf{v}_0 + \mu_2(\mathbf{b}_0 + \epsilon\nabla\times\mathbf{v}_0) + \mu_5\mathbf{e}_z + \mu_6 r\mathbf{e}_\varphi = 0, \quad (48)$$

$$\sim \delta\mathbf{A} : \nabla\times\mathbf{b}_0 + 2\mu_1\mathbf{b}_0 + \mu_2\nabla\times\mathbf{v}_0 = 0, \quad (49)$$

$$\sim \delta\mu_k : \quad I_1 = \pi l K,\ \hat{I}_2 = \pi l\hat{M},\ I_3 = \pi,\ I_4 = 2\pi\Omega_b,\ I_5 = \pi l u,\ I_6 = \frac{\pi l\Omega}{2}. \quad (50)$$

Equations (48) and (49) can be reduced to one equation for magnetic field

$$\epsilon\mu_2\nabla\times\nabla\times\mathbf{b}_0 + (1-\mu_2^2+2\epsilon\mu_1\mu_2)\nabla\times\mathbf{b}_0 + 2\mu_1\mathbf{b}_0 = 2\mu_2\mu_6\,\mathbf{e}_z. \quad (51)$$

A solution to this equation is the so-called double Beltrami flow,[19]

$$\mathbf{b}_0 = C_1\mathbf{b}_1 + C_2\mathbf{b}_2 + \frac{\mu_2\mu_6}{\mu_1}\mathbf{e}_z, \quad \nabla\times\mathbf{b}_{1,2} = \lambda_{1,2}\mathbf{b}_{1,2}, \quad (52)$$

where $\lambda_{1,2}$ are two roots of quadratic eigenvalue problem derived from homogeneous part of Eq. (51),

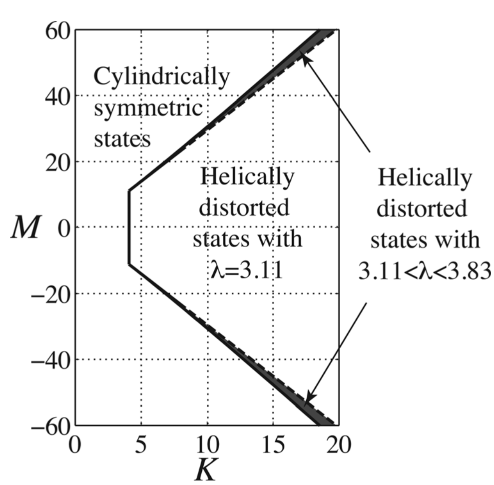

FIG. 8. Domains occupied by cylindrically symmetric and helically distorted MHD relaxed states [Eqs. (41)–(43)] in the plane $K-M$ (magnetic helicity−cross helicity). Grey areas correspond to helically distorted states with $3.11 < \lambda < 3.83$.

$$\lambda_{1,2} = \frac{-(1-\mu_2^2+2\epsilon\mu_1\mu_2) \pm \sqrt{(1-\mu_2^2+2\epsilon\mu_1\mu_2)^2 - 8\epsilon\mu_1\mu_2}}{2\epsilon\mu_2}. \quad (53)$$

The presence of two spatial scales associated with eigenvalues λ_1 and λ_2 is typical for the double Beltrami flows arising in the Hall MHD relaxation theory.[14,19,22,23]

Similar to single-fluid MHD case, the most general solution to Eqs. (48) and (49) satisfying constraints $I_3 = \pi$, $I_4 = 2\pi\Omega_b$, $I_5 = \pi l u$, $I_6 = \pi l\Omega/2$ is a superposition of cylindrically symmetric and helical modes,

$$\mathbf{A}_0 = \frac{r}{2}\mathbf{e}_\varphi + \sum_{j=1,2}\left[\frac{C_j}{\lambda_j}(J_1(\lambda_j r) - J_1(\lambda_j)r)\mathbf{e}_\varphi + \frac{C_j}{\lambda_j}(J_0(\lambda_j r) - J_0(\lambda_j))\mathbf{e}_z + \frac{\mathbf{H}_j}{\lambda_j}\right], \quad (54)$$

$$\mathbf{b}_0 = \nabla\times\mathbf{A}_0 = \mathbf{e}_z + \sum_{j=1,2}\left[C_j J_1(\lambda_j r)\mathbf{e}_\varphi + C_j\left(J_0(\lambda_j r) - \frac{2J_1(\lambda_j)}{\lambda_j}\right)\mathbf{e}_z + \mathbf{H}_j\right], \quad (55)$$

$$\mathbf{v}_0 = \Omega r\mathbf{e}_\varphi + u\mathbf{e}_z - \sum_{j=1,2}\frac{(\lambda_j+2\mu_1)}{\lambda_j\mu_2}\left[C_j\left(J_1(\lambda_j r) - \frac{4J_2(\lambda_j)}{\lambda_j}r\right)\mathbf{e}_\varphi + C_j\left(J_0(\lambda_j r) - \frac{2J_1(\lambda_j)}{\lambda_j}\right)\mathbf{e}_z + \mathbf{H}_j\right], \quad (56)$$

where $H_{1,2}$ are the helical parts of the solution, such that $\nabla\times\mathbf{H}_{1,2} = \lambda_{1,2}\mathbf{H}_{1,2}$, and the coefficients $C_{1,2}$ are

$$C_1 = -\frac{\lambda_1(\lambda_2+2\mu_1)(\mu_1+\mu_2\Omega_b)J_3(\lambda_2) + \lambda_1\lambda_2\mu_2(\Omega_b-\Omega)J_1(\lambda_2)}{\lambda_1(\lambda_2+2\mu_1)J_1(\lambda_1)J_3(\lambda_2) - \lambda_2(\lambda_1+2\mu_1)J_1(\lambda_2)J_3(\lambda_1)}, \quad (57)$$

$$C_2 = \frac{\lambda_2(\lambda_1+2\mu_1)(\mu_1+\mu_2\Omega_b)J_3(\lambda_1) + \lambda_1\lambda_2\mu_2(\Omega_b-\Omega)J_1(\lambda_1)}{\lambda_1(\lambda_2+2\mu_1)J_1(\lambda_1)J_3(\lambda_2) - \lambda_2(\lambda_1+2\mu_1)J_1(\lambda_2)J_3(\lambda_1)}. \quad (58)$$

Substituting these expressions into Eqs. (7), (8), and (11) we obtain the volume-averaged densities of the energy, the magnetic helicity and the generalized cross helicity,

$$\begin{aligned}\frac{E}{\pi l} = {} & \frac{1}{2} + \frac{u^2}{2} + \frac{\Omega^2}{4} - \frac{8C_1C_2(\lambda_1+2\mu_1)(\lambda_2+2\mu_1)J_2(\lambda_1)J_2(\lambda_2)}{\lambda_1^2\lambda_2^2\mu_2^2} \\ & + 2C_1C_2\left(1 + \frac{(\lambda_1+2\mu_1)(\lambda_2+2\mu_1)}{\lambda_1\lambda_2\mu_2^2}\right) \\ & \times\left(\frac{J_0(\lambda_2)J_1(\lambda_1) - J_0(\lambda_1)J_1(\lambda_2)}{\lambda_1-\lambda_2} - \frac{2J_1(\lambda_1)J_1(\lambda_2)}{\lambda_1\lambda_2}\right) \\ & + \sum_{j=1,2}\left[-\frac{4C_j^2J_2^2(\lambda_j)(\lambda_j+2\mu_1)^2}{\lambda_j^4\mu_2^2} + \left(1 + \frac{(\lambda_j+2\mu_1)^2}{\lambda_j^2\mu_2^2}\right)\right. \\ & \left.\times\left(\frac{C_j^2}{2}(2J_1^2(\lambda_j) - 3J_0(\lambda_j)J_2(\lambda_j) - J_2^2(\lambda_j)) + \frac{D_j}{2}\right)\right], \end{aligned} \quad (59)$$

$$K = \frac{C_1 C_2}{\lambda_1 - \lambda_2}(J_1(\lambda_2)J_3(\lambda_1) - J_1(\lambda_1)J_3(\lambda_2)) + \sum_{j=1,2}\left[\frac{2C_jJ_2(\lambda_j)}{\lambda_j} + \frac{2C_j^2}{\lambda_j}(J_2^2(\lambda_j) - J_1(\lambda_j)J_3(\lambda_j)) + \frac{D_j}{\lambda_j}\right], \tag{60}$$

$$\begin{aligned}\hat{M} = {}& u(1+\epsilon\Omega) - \frac{C_1C_2\mu_1(3+\mu_2^2-2\epsilon\mu_1\mu_2)}{\epsilon\mu_2^2} \times \left(\frac{J_0(\lambda_2)J_2(\lambda_1) - J_0(\lambda_1)J_2(\lambda_2)}{\lambda_1^2-\lambda_2^2} - \frac{8J_2(\lambda_1)J_2(\lambda_2)}{\lambda_1^2\lambda_2^2}\right)\\ &+ \sum_{j=1,2}\left[\frac{C_j(\lambda_j+\lambda_j\mu_2^2+2\mu_1)}{\lambda_j^2\mu_2^2}(\Omega J_2(\lambda_j) - uJ_3(\lambda_j)) + \frac{2uC_jJ_3(\lambda_j)}{\lambda_j} - \frac{(\lambda_j+2\mu_1)(\lambda_j+\lambda_j\mu_2^2+2\mu_1)}{\lambda_j^2\mu_2^3}\left(C_j^2\left(J_2^2(\lambda_j) - J_1(\lambda_j)J_3(\lambda_j) - \frac{J_2(\lambda_j)J_3(\lambda_j)}{\lambda_j}\right) + \frac{D_j}{2}\right)\right],\end{aligned} \tag{61}$$

where $D_{1,2}$ are magnitudes of the helical modes (note that helical eigenmodes of the curl operator corresponding to different eigenvalues $\lambda_1 \neq \lambda_2$ are orthogonal[29]),

$$D_{1,2} = \frac{1}{\pi l}\int \mathbf{H}_{1,2}^2 d^3\mathbf{r}.$$

Equations (60) and (61) with given K and M yield two conditions for determining two remaining unknowns. For a cylindrically symmetric state with $D_{1,2} = 0$ these unknowns are Lagrange multipliers μ_1 and μ_2 or, equivalently, λ_1 and λ_2, since they are related to μ_1 and μ_2 by Eq. (53). For a single-helicity state with $D_1 \neq 0$ and $D_2 = 0$, these unknowns are D_1 and λ_2 since eigenvalue λ_1 of the helical mode is specified now by Eq. (31). For a double-helicity state, the unknowns are D_1 and D_2 since both eigenvalues λ_1 and λ_2 (and, therefore, μ_1 and μ_2) are specified by Eq. (31).

The relaxed state found in such a way is not necessarily unique: for a given set of values of invariants there might be more than one solution corresponding to local minima of the energy functional. A true relaxed state should be selected as one of them with the lowest energy. One of the examples is illustrated in Fig. 9. It corresponds to the case when Eqs. (60) and (61) being solved for μ_1 and μ_2 yield multi-valued function $\mu_2(K, \hat{M})$ with point of condensation at $\mu_2 = 0$. Because of non-uniqueness of this solution there exists a discrete set of energy levels corresponding to given values of the invariants K and $\hat{M}$. The lowest energy state in Fig. 9 corresponds to $\mu_2 = 0$ and is independent of the value of generalized cross helicity $\hat{M}$. The dependence of energy E on magnetic helicity K for such state is shown in Fig. 10. Note that the non-uniqueness of the cylindrically symmetric states is a characteristic feature of the Hall MHD model, it has no practically important applications in the single-fluid MHD model.

Despite the complexity of Eqs. (57)–(61) a simple analytical treatment of them is possible when $\Omega_b = \Omega$, i.e., when boundary angular velocity defined by Eq. (15) is equal to averaged angular velocity defined by Eq. (17). In the rest of this section, we consider this case in more detail. The case $\Omega_b \neq \Omega$ is considered in Appendix.

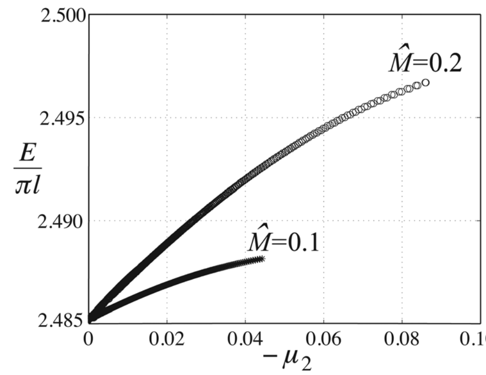

FIG. 9. Volume-averaged energy density as a function of Lagrange multiplier μ_2 for all possible cylindrically symmetric Hall MHD relaxed states [Eqs. (54)–(56)] satisfying constraints given by Eqs. (60) and (61). Results are presented for magnetic helicity $K = 2$, axial momentum $u = 0$, angular momentum $\Omega = 0$, boundary angular velocity $\Omega_b = 0$, Hall parameter $\epsilon = 0.1$, and two values of generalized cross helicity $\hat{M} = 0.1$ (stars) and $\hat{M} = 0.2$ (circles). The state with the lowest energy corresponds to $\mu_2 \to 0$ and is independent of value of $\hat{M}$.

When $\Omega_b = \Omega$ a state with the lowest energy corresponds to infinitely small μ_2 (Fig. 9). In order to show this, we assume that μ_2 is a small parameter and represent all quantities as a power series of μ_2. Then

$$\lambda_1 = -2\mu_1 - 2\mu_1\mu_2^2 + o(\mu_2^2) \sim 1,$$
$$\lambda_2 = -\frac{1}{\epsilon}\mu_2^{-1} + \frac{1}{\epsilon}\mu_2 + 2\mu_1\mu_2^2 + o(\mu_2^2) \sim \mu_2^{-1},$$

and

$$C_1 = \frac{\lambda_1}{2J_1(\lambda_1)} + o(1) \sim 1,$$
$$C_2 = -\frac{\lambda_1 J_3(\lambda_1)\mu_2^2}{2J_1(\lambda_1)J_3(\lambda_2)} + o(\mu_2) \sim \mu_2,$$

where it is also assumed that $C_2 \sim \mu_2$ (i.e., $J_3(\lambda_2) \sim \mu_2$), this assumption is justified below [see Eq. (68)]. Taking into account leading order terms in Eqs. (54)–(56), we arrive at

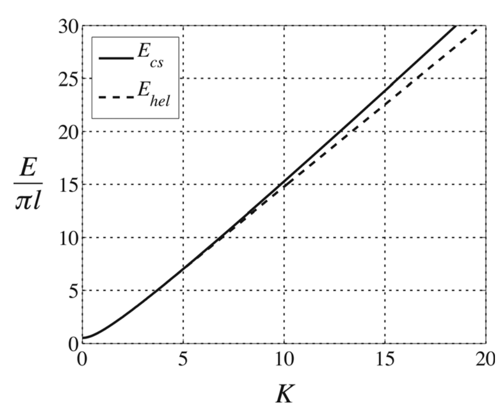

FIG. 10. Volume-averaged energy density of the Hall MHD relaxed state [Eqs. (54)–(56)] as a function of magnetic helicity K for cylindrically symmetric (solid curve) and helically distorted (dashed curve) solutions. Results are independent of generalized cross helicity $\hat{M}$. Other parameters are: axial momentum $u = 0$, angular momentum $\Omega = 0$, boundary angular velocity $\Omega_b = 0$, and Hall parameter $\epsilon = 0.1$. Note that for $K > 4.08$, the state with the lowest energy is helically distorted.

$$\mathbf{A}_0 = \frac{1}{2J_1(\lambda_1)}[J_1(\lambda_1 r)\mathbf{e}_\varphi + (J_0(\lambda_1 r) - J_0(\lambda_1))\mathbf{e}_z] + \frac{\mathbf{H}_1}{\lambda_1}, \tag{62}$$

$$\mathbf{b}_0 = \nabla \times \mathbf{A}_0 = \frac{\lambda_1}{2J_1(\lambda_1)}[J_1(\lambda_1 r)\mathbf{e}_\varphi + J_0(\lambda_1 r)\mathbf{e}_z] + \mathbf{H}_1, \tag{63}$$

$$\mathbf{v}_0 = \Omega r \mathbf{e}_\varphi + u\mathbf{e}_z - \frac{C_2}{\mu_2}[J_1(\lambda_2 r)\mathbf{e}_\varphi + J_0(\lambda_2 r)\mathbf{e}_z], \tag{64}$$

where helical mode $\mathbf{H}_2$ is neglected, since in order to be consistent with Eq. (61) its magnitude has to be $D_2 = o(\mu_2^3)$. Equations (62)–(64) demonstrate the separation of scales in a relaxed state: magnetic field varies slowly in radial direction (with typical scale $1/\lambda_1$) while velocity has fast varying part (with typical scale $1/\lambda_2$).

In the limit $\mu_2 \to 0$, Eqs. (59)–(61) become

$$\frac{E}{\pi l} = \frac{u^2}{2} + \frac{\Omega^2}{4} + \frac{\lambda_1^2}{4}\left(1 - \frac{J_0(\lambda_1)J_2(\lambda_1)}{J_1^2(\lambda_1)}\right) + \frac{\lambda_1 J_0(\lambda_1)}{4J_1(\lambda_1)} + \frac{D_1}{2}, \tag{65}$$

$$K = \frac{\lambda_1}{2}\left(1 - \frac{J_0(\lambda_1)J_2(\lambda_1)}{J_1^2(\lambda_1)}\right) + \frac{D_1}{\lambda_1}, \tag{66}$$

$$\hat{M} = u(1 + \epsilon\Omega) + \frac{\Omega J_2(\lambda_1)}{J_1(\lambda_1)} - \frac{2\epsilon|\mu_2|C_2^2}{\pi\mu_2^3}. \tag{67}$$

As one can see from Eq. (65) the fast varying part of the velocity does not contribute into energy in leading order. The energy of the relaxed state given by Eqs. (62)–(64) is the sum of kinetic part, which is due to uniform axial flow u and/or rigid azimuthal rotation Ω, and magnetic part, which is due to the force-free magnetic field with fixed magnetic helicity K. It is easy to verify that Eq. (65) yields the lowest possible value of the energy under constrained magnetic helicity, axial and angular momenta. This validates the use of the limit $\mu_2 \to 0$ (or, equivalently, $\lambda_2 \to \infty$).

In order to complete description of the relaxed state, one has to use Eq. (66) to determine λ_1 for cylindrically symmetric state (with $D_1 = 0$) or D_1 for helically distorted state [with λ_1 satisfying Eq. (31)]. Amplitude C_2 is then determined from Eq. (67),

$$C_2^2 = \frac{\pi\mu_2^2}{2\epsilon}\left|\hat{M} - u(1 + \epsilon\Omega) - \frac{\Omega J_2(\lambda_1)}{J_1(\lambda_1)}\right| \sim \mu_2^2, \tag{68}$$

which justifies assumption made above.

Though formally the terms in brackets in Eq. (64) are of order 1, they are negligible for any radius $r > 0$ in the limit $\lambda_2 \to \infty$. For large arguments $\lambda_2 r \gg 1$, Bessel functions entering Eq. (64) are bounded,

$$|J_m(\lambda_2 r)| \le \sqrt{\frac{2}{\pi|\lambda_2|r}} \to 0, \quad \lambda_2 \to \infty.$$

Therefore, at any fixed radius $r > 0$ the relaxed velocity is asymptotically close to

$$\mathbf{v}_0 = \Omega r \mathbf{e}_\varphi + u\mathbf{e}_z. \tag{69}$$

We should also note that the boundary value of azimuthal velocity from Eq. (69) is

$$v_\varphi\Big|_{r=1} = \Omega,$$

which is consistent with the assumed condition $\Omega_b = \Omega$. So, Eqs. (62)–(64) describe the lowest energy Hall MHD state satisfying all imposed constraints given by Eqs. (8), (11), and (14)–(17) with $\Omega_b = \Omega$.

Note that the relaxed magnetic field given by Eq. (63) is nothing else but a force-free Taylor state ($\nabla \times \mathbf{b}_0 = \lambda_1 \mathbf{b}_0$), i.e., it is a state with minimal magnetic energy under the constraints of constant magnetic helicity and total axial magnetic flux (Fig. 11). On the other hand, the asymptotic form of the relaxed velocity given by Eq. (69) is the flow, which minimizes kinetic energy with the constraints of constant axial and angular momenta. Thus, the Hall MHD relaxed state [Eqs. (62), (63), and (69)] can be found formally from the energy minimization procedure if one ignores the generalized cross helicity constraint.

This result is in agreement with the earlier considerations first made with the use of simple model in Ref. 20 and later for full Hall MHD model in Ref. 23. As mentioned there, it is a manifestation of the ill-posed variational problem: the constraint $\hat{I}_2$ (generalized cross helicity) is more "fragile" than the target functional E (energy), since $\hat{I}_2$ contains higher-order derivatives of velocity $\mathbf{v}$ in comparison with E. This result suggests that the relaxation in Hall MHD systems happens in such a manner as if there is no conservation of the generalized cross helicity. Such "fragility" of the generalized cross helicity in a real RFP experiment can be explained by its fast viscous decay due to an extra derivative of velocity and due to no-slip condition at the cylindrical boundary. The final relaxed state is trivial; it is the force-free magnetic field (Taylor state) and uniform axial flow and/or rigid rotation of plasma.

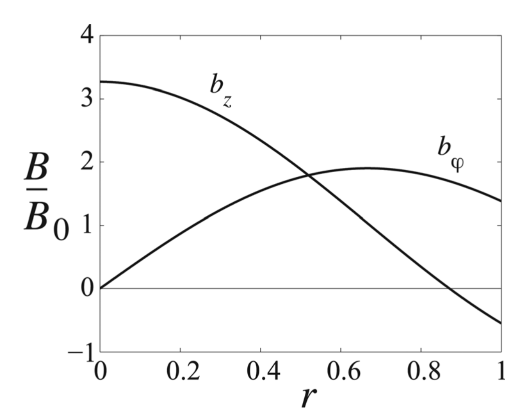

FIG. 11. Cylindrically symmetric Hall MHD relaxed state [Eqs. (54)–(56)] with the lowest energy, corresponding to a classical Taylor (force-free) state. The state is independent of generalized cross helicity $\hat{M}$. Other parameters are: magnetic helicity $K = 2$, axial momentum $u = 0$, angular momentum $\Omega = 0$, boundary angular velocity $\Omega_b = 0$, and Hall parameter $\epsilon = 0.1$. Note that such state has no flows since both momentum invariants u and Ω are zero.

From the mathematical point of view, obtained Hall MHD relaxed state corresponds to a single-fluid MHD relaxed state [Eqs. (23)–(25)] with $\mu_2 = 0$. Similar to single-fluid MHD case, helically distorted Hall MHD relaxed state can be oscillatory in time if $\mathbf{v}_0 \neq 0$. The non-cylindrical part of the relaxed magnetic field $\mathbf{H}_1$ is the helical wave with the wave-vector $\mathbf{k} = m/r\mathbf{e}_\varphi + k_z\mathbf{e}_z$ and the phase velocity $\mathbf{v}_{ph} = \mathbf{v}_0$, so the frequency of oscillations is [cf. Eq. (34)],

$$\omega = -\mathbf{k}\cdot\mathbf{v}_0 = -m\Omega - k_z u. \tag{70}$$

The transition of the force-free magnetic field to helically distorted state with $\lambda = 3.11$ occurs when magnetic helicity $K > 4.08$ [Sec. III A].

We stress here that the presence of the flow in the Hall MHD relaxed states is fully due to the inclusion of momenta invariants I_5 and I_6 into energy minimization procedure. If we ignore them to better adapt the model to the features of RFP experiments [see explanation in Sec. III B], the final Hall MHD state will be just force-free (Taylor) magnetic field with no plasma flows. Obviously, such state cannot explain the flows observed in RFP experiments.

V. COMPARISON WITH EXPERIMENT

In this section, we compare theoretically predicted relaxed velocity with the plasma velocity measurements in the Madison symmetric torus (MST) RFP experiment taken from Ref. 7. For comparison we use single-fluid MHD relaxed state [Eqs. (41)–(43)] from Sec. III B (with flow parallel to the force-free magnetic field), since it is obtained under assumptions consistent with realistic RFP experiment. As pointed out in Sec. IV, Hall MHD relaxed state under these assumptions does not have flows, so it cannot be used for comparison.

The MST RFP has a major radius $R = 1.5$ m and a minor radius $a = 0.5$ m; the other plasma parameters relevant to our study are as follows: the line-averaged density is $n \approx 1\times 10^{13}\ \mathrm{cm}^{-3}$, the plasma current is $I_p = 200-250$ kA, the reversal parameter is $F \approx -0.2$, and the pinch parameter is $\Theta \approx 1.7$.

MST plasmas exhibit quasiperiodic (sawtooth) oscillations, which are characterized by sudden bursts in all plasma diagnostics. Sawtooth oscillations in the MST consist of a fast crash phase ($\sim$0.1 ms) and a slow recovery phase ($\sim$3 ms). During the crash plasma relaxes towards its minimum energy state.[3,4] This relaxation event is accompanied by a rapid flattening of the plasma parallel momentum profile (Fig. 12).

In order to compare predictions of the relaxation theory with experimental observations presented in Fig. 12, we find parallel momentum normalized by the magnetic field using Eqs. (42) and (43),

$$q_{||} \equiv \frac{\mathbf{v}_0\cdot\mathbf{b}_0}{\mathbf{b}_0^2} = -\mu_2, \tag{71}$$

where μ_2 is constant independent of radius and can be calculated from Eq. (46). This result is in agreement with the observed flattening of the parallel momentum profile during relaxation events. The momentum profile flattening is mostly noticeable in the plasma core, while the changes at the edge are small (Fig. 12). This is similar to the incomplete relaxation of the parallel current profile observed in these relaxation events.[3]

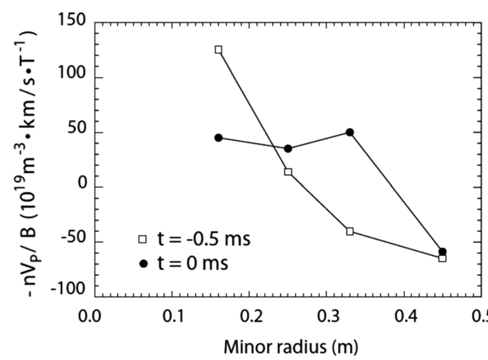

FIG. 12. Radial profile of the parallel momentum normalized by the magnetic field before (squares) and during (circles) the relaxation event in MST. Reprinted with permission from A. Kuritsyn, G. Fiksel, A. F. Almagri, D. L. Brower, W. X. Ding, M. C. Miller, V. V. Mirnov, S. C. Prager, and J. S. Sarff, Phys. Plasmas **16**, 055903 (2009). Copyright 2009, American Institute of Physics.

We emphasize that the relaxation theory is developed for isolated systems, while the MST experiment is an open system with external energy supply. However, even in open systems, where energy relaxation happens much faster than dissipative decay of the invariants, the principle of selective decay remains valid, and the present theory can be applied. This is the case of the MST RFP experiment, in which the characteristic energy relaxation time (crash phase, $t_{crash} \sim 0.1$ ms) is much shorter than the dissipation time ($t_{diss} \sim 100$ ms).

VI. CONCLUSION

In the present paper, the application of the Taylor relaxation theory to a cylindrical plasma pinch was generalized by inclusion into energy minimization procedure of velocity related ideal invariants. We obtained the minimum energy (relaxed) states within the framework of both single-fluid and Hall MHD. When we began the calculations, our motivation and expectation was that more general Hall MHD would lead to more diverse relaxed states than single-fluid MHD, and that these might help to explain the rotation that seems to be ubiquitous in the RFP experimental results. To our surprise, it was not so. It turned out that accurate minimization of the energy E in the Hall MHD model leads only to the force-free Taylor magnetic field and simple flows (rigid rotation and/or uniform axial flow), while MHD relaxed states are much more complex and diverse. Physically this suggests that the difference between two models appears in the process of relaxation in the way that makes Hall MHD states simpler. From the mathematical point of view, this is due to ill-posedness of the variational problem in the Hall MHD, which is related to "fragility" of the generalized cross helicity $\hat{I}_2$ explained at the end of Sec. IV. Our formal analysis shows that accurate energy minimizations in the Hall MHD with or without generalized cross helicity lead to the same result. Therefore, during Hall MHD relaxation in a weakly dissipative system one should expect rapid viscous decay of the generalized cross helicity—it is not a robust invariant and does not affect the final relaxed state.

In both single-fluid and Hall MHD models, depending on initial values of the corresponding invariants the relaxed states can be either cylindrically or helically symmetric. The interesting property of the helically symmetric relaxed states is their oscillatory behavior. The helical distortion of relaxed velocity and magnetic field acts as a helical wave, propagating on a cylindrically symmetric background. The phase velocity of such a wave is not zero only when the initial values of velocity related invariants are not zero.

Like all variational theories of plasma relaxation, the present calculation is silent as to the details of the dynamics that are responsible for the relaxation process. The only requirement is that they preserve the robust invariants assumed during the variational procedure. The comparison of the theoretically predicted relaxed states with MST RFP experiment (Sec. V) shows that the ideal single-fluid MHD results are in better qualitative agreement with the experimental data than the Hall MHD results. The single-fluid MHD yields more complex states with flow and agrees better with experimental results, than Hall MHD. The Hall effect (or other non-MHD effects) can influence the relaxation dynamics, but the final relaxed state in the experiment resembles the minimum energy state from the single-fluid MHD. Further insight in this regard requires more detailed experimental measurements and large scale computer simulations.

ACKNOWLEDGMENTS

The authors wish to thank C. Hegna and C. Sovinec for useful discussions. This work is supported by the National Science Foundation and by the U.S. Department of Energy under Grant DE-FG02ER-54868.

APPENDIX: RELAXED STATES IN HALL MHD FOR $\Omega_b \neq \Omega$

In general case, when $\Omega_b \neq \Omega$, there are no simple analytical solutions to Eqs. (57)–(61). In order to find, for example, a cylindrically symmetric relaxed state (so, $D_{1,2} = 0$), one has to solve Eqs. (60) and (61) for μ_1 and μ_2 (or, equivalently, for λ_1 and λ_2), substitute found values into Eqs. (57)–(59), and if there are several solutions, choose the state with the lowest energy. Such procedure can be realized numerically and it leads to non-trivial profiles of magnetic field and velocity (Fig. 13). It should be emphasized here that the non-trivial relaxed states obtained in this way do not always have a smooth transition to a trivial state [Eqs. (62), (63), and (69)] when $\Omega_b \to \Omega$.

We note that the Lagrange multipliers method applied to a minimization problem with constraints gives a solution from a class of continuous, differentiable functions. If we are not restricted to this class of functions, it is possible to construct a discontinuous relaxed state, which has lower energy than any other state. Indeed, let us represent velocity in the form,

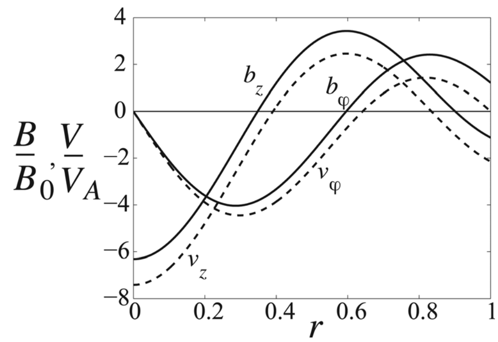

FIG. 13. Example of a "smooth" cylindrically symmetric Hall MHD relaxed state [Eqs. (54)–(56)], which is not a true minimum energy state. Calculations are done for magnetic helicity $K = 2$, generalized cross helicity $\hat{M} = 0.1$, boundary angular velocity $\Omega_b = 0$, axial momentum $u = 0$, angular momentum $\Omega = 0.1$, and Hall parameter $\epsilon = 0.1$. Solid lines are components of magnetic field and dashed lines are components of velocity.

$$\mathbf{v} = \mathbf{u} + (\Omega_b - \Omega)S(r)\mathbf{e}_\varphi, \tag{A1}$$

where $\mathbf{u}$ is assumed to be spatially continuous and $S(r)$ is a discontinuous function describing a spike at the boundary,

$$S(r) = \begin{cases} 0, & r \neq 1; \\ 1, & r = 1. \end{cases}$$

For such representation of velocity, the generalized cross helicity constraint now has a form,

$$\hat{I}_2 = \int \mathbf{u} \cdot \left(\mathbf{b} + \frac{\epsilon}{2}\nabla \times \mathbf{u}\right) d^3\mathbf{r} + \pi l \epsilon (\Omega_b - \Omega) u_z \Big|_{r=1}, \qquad \hat{I}_2\Big|_{\tau=0} = \pi l \hat{M}, \tag{A2}$$

and the azimuthal component of $\mathbf{u}$ should satisfy boundary condition [cf. Eq. (15)],

$$\int_0^{2\pi} u_\varphi \Big|_{r=1} d\varphi = 2\pi\Omega. \tag{A3}$$

In terms of continuous differentiable functions $\mathbf{b}$ and $\mathbf{u}$, the problem is now reduced to the case $\Omega_b = \Omega$ with modified generalized cross helicity [Eq. (A2)]. Hence, continuous part of the relaxed state is determined by Eqs. (62), (63), and (69). The spike discontinuity at the boundary introduced in Eq. (A1) enters the azimuthal component of the relaxed velocity,

$$\mathbf{v}_0 = \Omega r \mathbf{e}_\varphi + u\mathbf{e}_z + (\Omega_b - \Omega)S(r)\mathbf{e}_\varphi. \tag{A4}$$

The state given by Eqs. (62), (63), and (A4) has the lowest possible energy under imposed constraints. Therefore, isolated dissipative Hall MHD system will tend to relax toward this state.

A discontinuity at the boundary in the relaxed azimuthal velocity Eq. (A4) is due to the assumption that axial flux of the fluid vorticity I_4 [Eq. (15)] is conserved. However, similar to the generalized cross helicity, this constraint is more "fragile" than the energy since it contains higher-order derivatives of the velocity. As a result, ideal invariant I_4 is more susceptible to dissipation than energy and cannot be considered as a constant during relaxation. Ignoring this invariant in the energy minimization procedure, we obtain Eq. (69) for the relaxed velocity without any discontinuities.

The relaxed state obtained in such way is exactly the state described by Eqs. (62), (63), and (69), and all results of Sec. IV also apply. So, the final relaxed state of the cylindrical pinch in the Hall MHD is always a trivial state with the force-free magnetic field (Taylor state) and uniform axial flow and/or rigid rotation of plasma.

[1] J. B. Taylor, Phys. Rev. Lett. **33**, 1139 (1974).
[2] J. B. Taylor, Rev. Mod. Phys. **58**, 741 (1986).
[3] S. Ortolani and D. D. Schnack, *Magnetohydrodynamics of Plasma Relaxation* (World Scientific, Singapore, 1993).
[4] H. Ji, S. C. Prager, and J. S. Sarff, Phys. Rev. Lett. **74**, 2945 (1995).
[5] C. D. Cothran, M. R. Brown, T. Gray, M. J. Schaffer, and G. Marklin, Phys. Rev. Lett. **103**, 215002 (2009).
[6] C. D. Cothran, M. R. Brown, T. Gray, M. J. Schaffer, G. Marklin, and V. S. Lukin, Phys. Plasmas **17**, 055705 (2010).
[7] A. Kuritsyn, G. Fiksel, A. F. Almagri, D. L. Brower, W. X. Ding, M. C. Miller, V. V. Mirnov, S. C. Prager, and J. S. Sarff, Phys. Plasmas **16**, 055903 (2009).
[8] J. M. Finn and T. M. Antonsen, Phys. Fluids **26**, 3540 (1983).
[9] K. Chiyoda, J. Phys. Soc. Jpn. **55**, 1139 (1986).
[10] W. Schuurman and M. P. Weenink, J. Phys. Soc. Jpn. **55**, 4574 (1986).
[11] J. Shiraishi, S. Ohsaki, and Z. Yoshida, J. Plasma Fusion Res. Ser. **6**, 169 (2004).
[12] R. Horiuchi and T. Sato, Phys. Fluids **31**, 1142 (1988).
[13] R. N. Sudan, Phys. Rev. Lett. **42**, 1277 (1979).
[14] L. Turner, IEEE Trans. Plasma Sci. **PS-14**, 849 (1986).
[15] K. Avinash and J. B. Taylor, Comments Plasma Phys. Controlled Fusion **14**, 127 (1991).
[16] L. C. Steinhauer and A. Ishida, Phys. Rev. Lett. **79**, 3423 (1997).
[17] L. C. Steinhauer and A. Ishida, Phys. Plasmas **5**, 2609 (1998).
[18] C. C. Hegna, Phys. Plasmas **5**, 2257 (1998).
[19] S. M. Mahajan and Z. Yoshida, Phys. Rev. Lett. **81**, 4863 (1998).
[20] Z. Yoshida and S. M. Mahajan, Phys. Rev. Lett. **88**, 095001 (2002).
[21] L. C. Steinhauer, H. Yamada, and A. Ishida, Phys. Plasmas **8**, 4053 (2001).
[22] L. C. Steinhauer, Phys. Plasmas **9**, 3767 (2002).
[23] S. Ohsaki and Z. Yoshida, Phys. Plasmas **12**, 064505 (2005).
[24] R. Numata, Z. Yoshida, and T. Hayashi, Comp. Phys. Comm. **164**, 291 (2004).
[25] R. Numata, Z. Yoshida, and T. Hayashi, J. Plasma Fusion Res. Ser. **6**, 130 (2004).
[26] H. P. Furth, J. Killeen, and M. N. Rosenbluth, Phys. Fluids **6**, 459 (1963).
[27] A. Reiman, Phys. Fluids **24**, 956 (1981).
[28] A. Reiman, Phys. Fluids **23**, 230 (1980).
[29] Z. Yoshida and Y. Giga, Math. Z. **204**, 235 (1990).